Optica Applicata, Vol. XXXII, No. 4, 2002

Application of the quantitative analysis of interferograms in describing the acoustic features of the electro-acoustic transducer

Piotr Perz, Jarosław Stańko

Institute of Acoustics, Adam Mickiewicz University, ul. Umultowska 85, 61–614 Poznań, Poland.

A method of converting the striae pattern registered on the interferogram of an examined object into the adequate vibration amplitude pattern, which enables calculation of the acoustic pressure radiation, is presented. The range of the method application has been discussed.

1. Introduction

A hologram record of the vibrating object enables obtaining fringe patterns, on the basis of which the vibration amplitude can be defined [1]. In practice, mainly the qualitative analysis of the holograms takes place, *i.e.*, the surface vibration character is defined (location of the nodal areas, definition of the vibration symmetry, *etc.*). The quantitative analysis enabling one to obtain exact values of the amplitude pattern on the surface under examination is carried out relatively seldom, which is due to the experimental difficulties connected with photometering, as well as with the necessity of designing a special programme converting the brightness pattern registered during photometering into the amplitude pattern. This research presents the converting procedure of the fringe pattern brightness into the amplitude pattern, on the basis of which the acoustic pressure generated by the examined electro-acoustic transducer is calculated. The research also discusses the basic limitations of the method in question, claiming that their source can be found in the very method, as well as in the analysing equipment resolution (CDD camera).

2. Quantitative analysis of the holographic images

The transformation process of a holographic image of a vibrating object into the values defining the acoustic features of the object can be divided into three phases: 1 – registration of the light intensity pattern on the object surface; 2 – converting the light intensity value into the vibration amplitude pattern on the object surface; 3 – calculation of the generated acoustic pressure.

In the first phase, we register the brightness pattern in the interferogram of the vibrating object; this process, in the case of reflection holograms can be used effectively only with the application of TV [2]. In the second phase, the registered brightness pattern is converted into the amplitude pattern. Generally, the equation relating the intensity $I(x, y)$ of the light reflected from the vibrating surface to the amplitude d is used [1]

$$I(x, y) = I_0(x, y)F(d\gamma) \tag{1}$$

where $I_0(x,y)$ – light intensity recorded for the non-vibrating object; x, y – coordinates of the object surface. The factor γ depends on the geometry of the meter system and on the wavelength of the light used for the registration. The function F in Eq. (1) depends on the choice of the hologram registration method and it takes the form of cosine in the case of the double exposure method, and J_0 (Bessel's function of the first type, zero order) in the case of the time averaged method. It should be noted that the dependence of the light intensity and the vibration amplitude is a multi-dependence (which results from the form of the F function, independent of the way the hologram is registered). This causes that the programme calculating the vibration amplitude cannot be only a programme for simple multiplication of the light intensity value by a given factor. For hologram registration in acoustic research the method of the time average is used most often, which makes it easier to interpret the holograms – maximum brightness decays with an increase in vibration amplitude.

Holographic interferometry enabling visualisation of the vibration pattern was a great facilitation as regards acoustic problems [5]. Striae enable mapping of the surface vibration, however, contrary to an ordinary map, they are not marked (no value is assigned to them). In order to use it quantitatively, an interferogram needs additional calibration. This process depends on the recording mode. For the double exposure fringes join places of equal deflection value, the location of the nodal areas is not however defined, it depends on the experimentator and his knowledge of physics of the phenomenon under investigation. It can be said that to a well-defined pattern of mutual deflection variation, the experimentator adds a constant ingredient – calibration. Some inconvenience resulting from the double exposure itself must be taken into account, *i.e.*, the results are dependent on the choice of the exposure moments. From the acoustic point of view, it is not easy to choose the exposure moments so as to arrive at maximal and minimal deflection of the surface examined (it is impossible when assuming the phase difference between given points of the diaphragm). On the whole, it is relatively easy to count the fringes with this method, but it is more difficult to interpret the results. In the time averaged method the definition of the nodal area location is immediate. Fringes depend not on the difference between deflections in the exposures, but they are function-dependent on the amplitude of the vibration, so they represent the value of the vibration amplitude.

In normal applications making an interferogram with the use of the time averaged method is much easier, so it is natural to aim at gaining some numerical data on this basis. In this research it has been proved that gaining such data is possible, however it attracts additional simplifying assumptions. These results can be useful in acoustic research.

In the third phase, the value of the acoustic pressure p generated by a given vibration pattern on the surface of the transducer S is calculated. This phase is based on the use of the Rayleigh–Kirchhoff formula [3]

$$p = -\rho\omega^2 \int_S \frac{d(x,y)\exp[(\Phi(x,y) - kr_{x,y})i]}{2\pi r_{x,y}} \mathrm{d}S \tag{2}$$

where: $d(x,y)$ – amplitude of displacement of surface point x, y; ρ – medium (air) density; k – wave number; $\Phi(x,y)$ – phase of displacement of surface element x, y; ω – angular frequency; $r_{x,y}$ – distance between point (x,y) on the vibrating surface S and point of observation.

3. Calculation procedure – analysing programmes

The holographic image (time averaged method) of an object vibrating with a given frequency has been recorded on the IBM computer with the use of the CDD camera and the "frame-graber" system of the resolution of 256×256 lines and dynamics of 256 grey levels. The part directly concerning the transducer under examination was removed from the whole image, in order to avoid any deformations connected with the unequal background illumination. Giving the images behind the transducer maximum brightness caused the calculating programme to assume automatically zero vibration amplitude for these areas. The calculating programme then transferred the data gained in this way describing the brightness pattern on the transducer surface into the amplitude pattern. The programme worked as follows: on the transducer diaphragm the nodal areas were defined, then, on the basis of continuity rule of the vibration pattern variation, the brightness minima were found and assigned successive minimum arguments of the Bessel's function (Eq. (1)). It enabled (with the knowledge of geometric configuration of the diaphragm) the definition of the vibration amplitude on the transducer diaphragm. This data could form the basis of a programme calculating, with the use of Eq. (2), the acoustic pressure in the transducer axis and its directional characteristics. It should be noted that the above mentioned ambiguity of the Bessel's function makes it necessary to make an additional assumption of the continuity of the amplitude pattern variation (the "smoothness" of the diagram). In practice, this assumption is always true, however, the programme discussed does not allow the analysis of the vibration pattern on the surface of the transducer with the diaphragm of free outer suspension. Due to the limitations of the method of hologram recording (time averaged method) applied here it was impossible to define the sign (phase) of the vibration. Thus, two calculation variants were considered: 1 – vibration on the whole diaphragm surface takes place in the same phase (piston vibration); 2 – neighbouring areas separated by the nodal areas vibrate in the anti-phase (180°) [5].

The definition of the border brightness values assigned to the appearance of the nodal areas was a problem, experimental in nature and influencing the results obtained. Formula (1) combines the intensity of the light reflected from the non-vibrating object with the intensity coming from the object undergoing the changes (examined). The intensity pattern coming from the non-vibrating object surface is usually complicated, and the record of this pattern must be made separately from the record of the vibrating one – there are difficulties with keeping the same light conditions, and thus there is a probability that mistakes may occur. In order to simplify calculation in the programme, the intensity I_0 was assumed constant on the whole surface under investigation. The light intensity value was assigned arbitrarily before the calculation started. This solution influenced only the definition of the location of the nodal areas, however, with reference to the assumed system of defining the vibration location of the non-zero amplitude, it did not influence that part of the calculation. Taking into consideration the simplifications discussed, the goal of this research was not only to check the working (possibilities) of the calculation procedures, but mostly their influence on the correctness of the gained results.

To sum up, the following simplifying assumptions were made during the calculation [6]:

- constant value of brightness on the transducer surface (in non-vibrating state);
- flat transducer surface;
- surface vibrations being either homogenous or in the anti-phase;
- vibrations parallel to the sensitivity vector.

4. Research results

A mid-tweeter loudspeaker TONSIL GD 16/25 was examined. The interferograms of the speaker diaphragm were recorded (with the time averaged method) in a standard holographic system for the driving signal frequencies: 1400 Hz, 2 kHz, 3 kHz, 4600 Hz, 5 kHz, 5900 Hz, 7 kHz. The driving signal frequency was chosen on the basis of the transducer transfer function (Fig. 1) so as to cover the whole bandwidth of the transducer. The loudspeaker driving signal voltage equalled 150 mV for the signals of 1400–5000 Hz; for the remaining frequencies (considering very small vibration amplitude comparable with the resolution of measuring method) the driving signal voltage was 250 mV. During the hologram recording process the loudspeaker was mounted in 50 cm × 50 cm wooden baffle. The illumination and beam and observation axis were adjusted in such a way that the sensitivity vector was parallel to the main

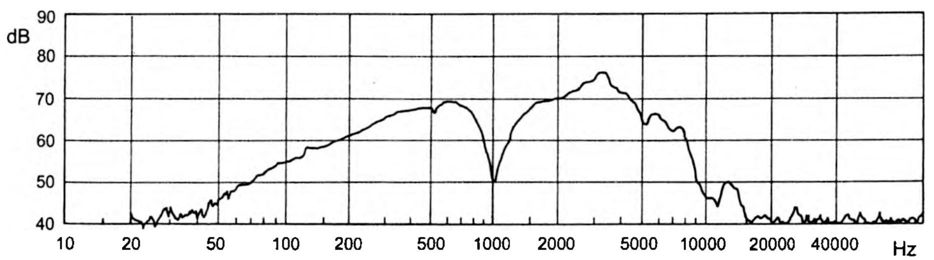

Fig. 1. Transfer function of the loudspeaker under investigation.

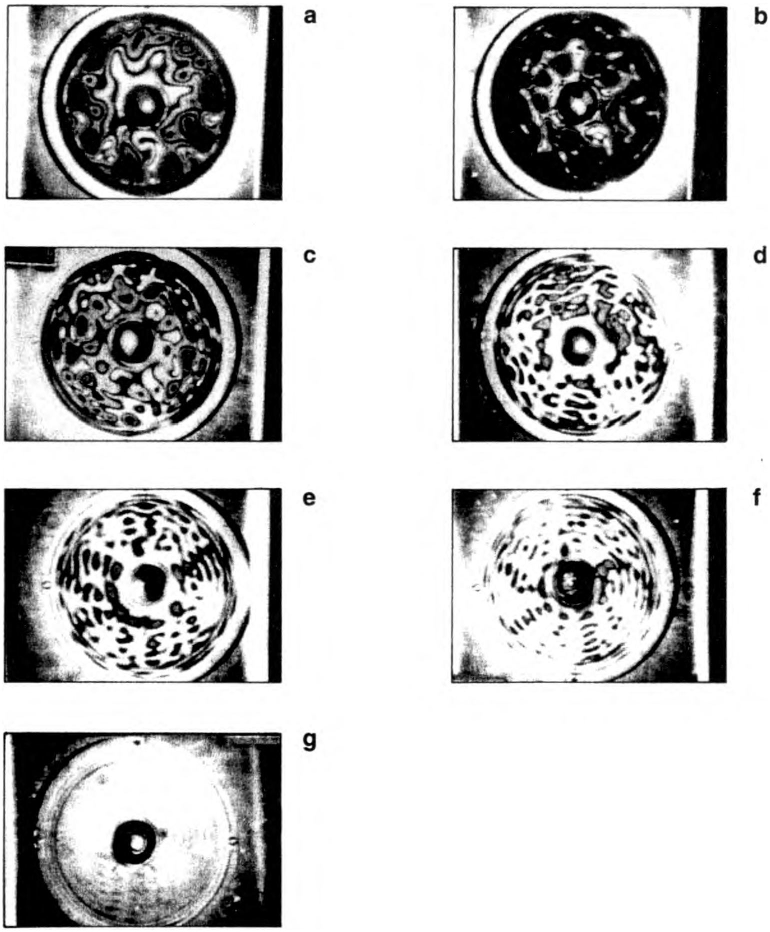

Fig. 2. Interferograms of the loudspeaker diaphragm for the driving signal frequency and amplitude: 1.4kHz, 150 mV (**a**); 2 kHz, 150 mV (**b**); 3 kHz, 150 mV (**c**); 4.6 kHz, 150 mV (**d**); 5 kHz, 150 mV (**e**); 5.9 kHz, 250 mV (**f**); 7 kHz, 250 mV (**g**).

loudspeaker axis. Loudspeaker semiapex angle was equal 60°, and finally Eq. (1) factor $\gamma = 2\pi/\lambda$. Photos of the interferograms are presented in Fig. 2. For low frequencies of the driving signal (Fig. 2**a**, **b**), a differentiation of the vibration pattern can be observed on the diaphragm surface as well as nodal areas. It can be said, however, that these are in fact piston vibrations, *i.e.*, the division into areas vibrating in the anti-phase on the diaphragm does not occur. For the driving frequency of 3 kHz (and higher) on the external part of the diaphragm there appear bending waves; according to the theory [4], [5] it should be assumed that neighbouring anti-nodal areas vibrate in the anti-phase. Together with an increase in driving frequency we can observe an increase in the nodal areas number, moving of the transition circle (the border dividing, on the diaphragm surface, areas of the flexural-inner waves domination and of bending-outer ones) [5] in the direction to the diaphragm centre, as well as a decrease in the deflection amplitude in anti-nodal areas. It should be noted that for the exciting frequency of 7 kHz (Fig. 2**g**) the vibration amplitude is so small that it is almost comparable with the resolution of the method.

Holographic images (for given driving signal frequency) were recorded on IBM AT computer with the use of the "frame-graber" card. The data obtained were used (according to the above discussed schema) for calculating the vibration amplitude pattern on the transducer surface. Some examples of amplitude distribution computed on the basis of fringe patterns are shown in Fig. 3. For low frequency of driving force (Fig. 3**a**) we observe different amplitude values but no phase changes across the diaphragm surface. For higher frequencies, 4600 Hz (Fig. 3**b**) and 5900 Hz (Fig. 3**c**), phase changes as well as amplitude value changes are visible. Amplitude patterns as shown in Fig. 3 were computed for all interferograms and then, on their basis the acoustic pressure generated by the transducer for given frequency was calculated. The pressure values on the transducer axis were calculated according to formula (2). The method of hologram recording (time averaged method) enables expression of the dependences between the light intensity and the vibration amplitude (Eq. (1)), however, it does not allow defining the sign (phase) of vibration. In the calculations, a variant in which vibration on the whole surface took place in the same phase was assumed (results are presented in Fig. 4 with the use of triangles), as well as the variant assuming that two neighbouring areas vibrate in the anti-phase (180°) [4], [5] – the results are presented in Fig. 4 with the use of filled squares. The results of the acoustic

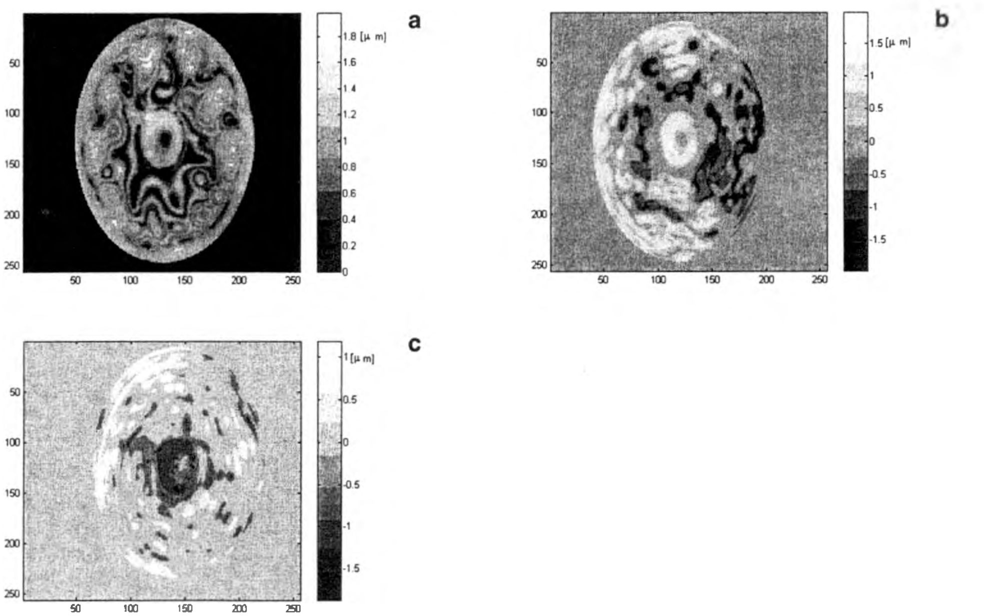

Fig. 3. Examples of amplitude distribution computed on the basis of interferograms (X, Y axes – in pixels, brightness scaled in micrometers); 1400 Hz (**a**); 4600 Hz (**b**); 590 Hz (**c**).

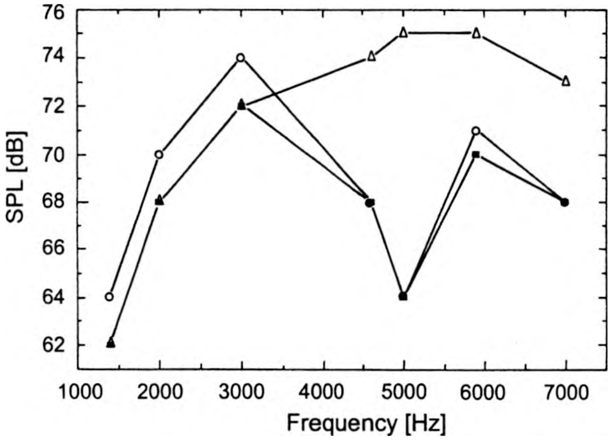

Fig. 4. Sound pressure levels (SPL) calculated and measured (–○– acoustical measurment, –■– with phase difference, –△– uniform phase distribution).

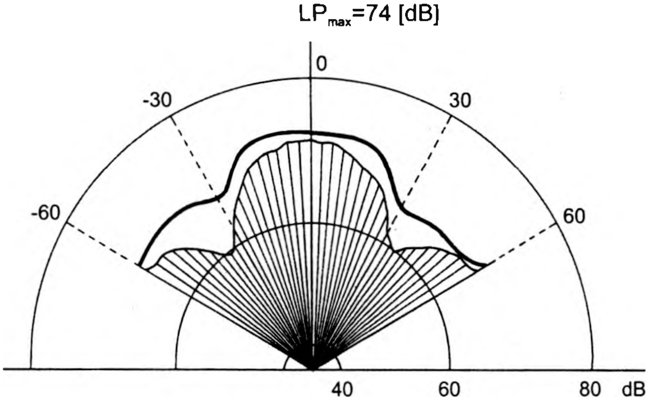

Fig. 5. Directional characteristics of the loudspeaker, calculated (thin line) and measured (thick line). Driving signal frequency 3 kHz.

measurements are marked in Fig. 4 with the use of open circles – the values of the acoustic pressure level were measured when the loudspeaker was activated by signals with the frequencies and amplitudes adequate to the parameters of the signals for which the holograms were made. Acoustic measurements were performed in the anechoic chamber, the loudspeaker was mounted in a baffle in order to avoid the influence of back radiation on the results [4].

In Figure 5, a comparison of the directional characteristics of the transducer is presented for the frequency of 3 kHz, calculated (thin line) and measured (thick line). Since the calculating programme did not include the diffractional effects, the calculations were done only in the angle range not exceeding the apex angle of the loudspeaker diaphragm.

5. Discussion of results, limitations to the method

Comparing the diagrams of the calculated and measured acoustic pressure (Fig. 4) indicates that they are similar for the frequencies of the activating signal not higher than 3 kHz. In terms of higher frequencies of the activating signal the results gained, assuming the lack of phase differences of the individual areas (divided by the nodal areas), significantly exceed the values gained by the assumption that the divided areas vibrate in the anti-phase. This pattern results from the characteristics of the diaphragm vibration of the transducer – for the frequency below 3 kHz (Fig. 2**a**–**c**) no nodal areas are observed; however they appear for the higher frequencies. Thus, in the areas of low frequencies both variants are in fact identical, the differences appear for higher frequencies. The comparison of the calculated results with the acoustic measurement results allows us to claim definitely that the variant assuming the existence of the separated areas vibrations in the anti-phase is the correct one. This result is not surprising, it comes from the vibration theory [5], however high agreement of the calculated results (assuming the phase difference 180°) with the results of the acoustic measurements allows us to claim that the damping in the diaphragm material is very little [7], this result (as it seems) can be spread on other cellulose diaphragms.

Quantitative differences for lower frequencies between the calculated and measured levels of the acoustic pressure result mainly from too low resolution of the "frame-graber" card, since low frequencies fringes are located so close to one another that after digitalisation they flow together and thus introduce errors into the calculating programme of the vibration amplitude. For higher frequencies the striae density decreases (Fig. 2**d**–**g**), which results in a decrease in the difference.

A comparison of the directional characteristics (measured and calculated) indicates that together with increasing the measurement angle (with respect to the main axis of the transducer) the difference between these values increases. It can also be claimed that the minima of the directional characteristics are moved in the direction of the main axis. The reason for that seems to be the assumption in the calculations that the surface of the transducer is flat, while in fact the transducer examined was a cone with an apex angle of 120°.

Formula (1) combines the intensity of the light reflected from the non-vibrating object with the light intensity coming from the object subject to changes (examined). The brightness pattern coming from the non-vibrating object is usually complicated, moreover, its record must be done separately from the record of the vibrating object; there appear difficulties in assuring the same light conditions, so there is a great risk of mistake occurrence. In the calculating programme, in order to simplify calculations, it was assumed that the intensity I_0 is constant, independent of the surface point. The light intensity value was assumed arbitrarily before the calculation started. The assumption of this solution influenced the definition of the location (extensiveness) of the nodal areas, and thus it could influence those values of the calculated levels of the acoustic pressure.

6. Conclusions

Analysing the results presented in this research we can claim that there is a certain range of vibration amplitudes and transducer values for which it is possible to convert the striae brightness pattern into deflection pattern, and further, to calculate the acoustic pressure generated by the object under examination. These calculations are exact, despite some simplifying assumptions aiming at acceleration of the calculation process. One of these assumptions is a thesis that the diaphragm vibrations are parallel to the sensitivity vector only, which is, of course, untrue; it should be assumed that these vibrations are perpendicular to the diaphragm surface. However, in the case where vectors of observation and illumination are almost identical with the axis of the analysed diaphragm, this assumption is reduced to a change of the absolute value of the amplitude only, the scale factor is homogeneous on the whole surface of the diaphragm, and it can be included, for example, through a choice of the reference pressure value in the programme calculating the level of the generated sound.

The results allow us to claim that it is possible to convert the light intensity pattern of an interferogram (obtained by the time averaged method) of vibrating objects into the value of acoustic pressure generated by this object.

A comparison of the results calculated by the above-mentioned method with the values of the acoustic measurements indicates their good agreement. It means that the simplifying assumptions during the calculations are true – at least with respect to cone cellulose diaphragms.

This results may be applied in, for example, calculations of the contribution of individual parts of a diaphragm to its total radiation.

Acknowledgments – This work was partly supported by the State Committee for Scientific Research (KBN), Poland, under the grant No. 7 TO7B 028 13.

References

[1] CATHEY W.T., *Optical Information Processing and Holography* (in Polish), PWN, Warszawa 1978.
[2] HOJAN E., PERZ P., Frequenz **38** (1984), 85.
[3] SHINDO T., YASHIMA O., SUZUKI H, J. Audio Eng. Soc. **28** (1980), 490.
[4] Polish Standart PN-EN 60268-5, Sound System Equipment – Part 5: Loudspeakers (1998)
[5] FRANKORT F., J. Audio Eng. Soc. **26** (1978), 609.
[6] PERZ P., STAŃKO J., *Quantitative analysis of interferograms as a tool for determining of acoustical parameters of electroacoustic transducer*, [In] XLV Open Seminary of Acoustics, Poznań 1998, pp. 499–504 (in Polish).
[7] DOBRUCKI A., *Numerical modelling of the moving system of electrodynamic loudspeaker* (in Polish), [In] Scient. Papers of the Institute of Telecommunication and Acoustics of the Technical University of Wrocław, No. 70, (1992).

Received January 28, 2002
in revised form July 31, 2002